Analytical Comparison of Various Fiber-Optic CDMA Receiver Structures

Sina Zahedi, *Student Member, IEEE,* and Jawad A. Salehi, *Member, IEEE*

Abstract—In this paper, we study the performance of optical code-division multiple access (CDMA) systems using various receivers structures. Two general classes of receivers based on required electronic bandwidth are studied. Optical orthogonal codes (OOCs) are utilized as signature sequences and the performance studied in this paper takes into account the effect of all major noise sources, i.e., quantum shot-noise, dark current noise, and Gaussian circuit noise. Furthermore, this paper introduces a generalized method of analyzing the performance of various optical CDMA receiver structures. Required mean number of photon count per chip time for reliable transmission of data bits for various receiver structures is investigated. Finally, the advantages and disadvantages of various receiver structures are discussed.

Index Terms—Channel interference, optical code division multiple access (CDMA), optical encoder and decoder, optical hard-limiter, Poisson distribution.

I. INTRODUCTION

IN recent years, there has been a tendency toward the use of spread spectrum techniques in fiber-optic multiple-access networks. This is mainly because of vast bandwidth availability in fiber-optic medium. This bandwidth is known to be much higher than the bandwidth of all studied electronic detection and processing techniques. A spread spectrum technique can use this excess bandwidth as the required processing gain to provide multiple access capability to the network. A spread spectrum multi-access system, using optical orthogonal codes (OOCs) as spreading codes, was proposed in [1] for intensity modulation/direct detection OOK optical signals. Performance analysis of such systems with various receiver structures was the subject of many articles [2], [5]–[7]. Salehi and Brackett [2] analyzed the system performance taking into account channel interference and have shown the usability of OOCs in ideal interference limited cases. They have suggested the use of an optical hard-limiter to suppress some interference patterns that are capable of producing errors and have shown the improvement in system performance due to multi-user interference. They have suggested alternative receiver designs, which differ on the speed of electronic circuitry required in the receiver. However, in their analysis assuming only channel interference, performance of these receivers are the same, but their performances differ if we consider other noise sources. Kwon [9] has analyzed the performance of a correlation receiver with and without a hard-limiter in a system using an Avalanche Photo Diode (APD) by modeling the received signal as a Gaussian Process. His analysis is the first attempt to consider various noises and imperfections in these systems. However, it has been shown that the use of Gaussian approximation for PIN diode receivers may not be an acceptable approximation especially when one considers low-power optical signals. He has shown that the use of hard-limiter before correlation receiver improves the performance of the receiver slightly. Ohtsuki [7] has proposed the use of double optical hard-limiter to realize the optical AND gate structure [8] and has shown that the system performs well in the presence of Photodetector Poisson Shot-Noise. Shalaby [6], on the other hand, has introduced the concept of chip-level detection in optical CDMA networks. His analysis also considers the Poisson Shot-Noise. However, it will be shown in this paper that Quantum-Limit anticipations are not good predictions of the system performance when considering other noise sources such as dark current and circuit thermal noise and the closeness of results will depend on the receiver structure and noise power.

In this paper, we present a unified model for performance analysis of different proposed receiver structures taking into account all major noise sources, i.e., quantum shot-noise, photodetector dark current noise, and circuit Gaussian noise. The analysis performed here simplifies for special cases to the analysis performed in preceding analyses, especially those in [6] and [7]. We will discuss the major strengths and drawbacks of each structure. Our analysis is based on photon-counting techniques, which is proved to give the best bit error rate (BER) predictions. For numerical computation of results, we avoid the common Gaussian approximations. However, since the number of effective parameters in BER (such as noise and interference terms) is high, numerical calculation of bit error probability is quite intractable. For that reason, we used saddle-point approximation techniques for BER evaluation of these systems, which relies on characteristic function of the received decision criteria.

Section II of this paper presents the basics of photon-counting techniques. Section III gives a description of proposed CDMA system using OOC codes and introduces different receiver structures. In Section IV, we present BER analysis of different receiver structures and Section V uses the saddle-point approximation technique for numerical evaluation of BER and gives the numerical results and conclusions.

II. STATISTICAL CHARACTERISTICS OF PHOTON-COUNTING

A photodetector with quantum efficiency η can be modeled as a random partitioner with probability η. Each incoming photon has a probability η to be detected, i.e., η is the probability that an incoming photon releases an electron in photodetector. If the input process to a random partitioner is one of the common light processes such as Poisson, Bose-Einstein, or Laguerre, then the statistics of output process can be shown to be the same with average of the distribution multiplied by η. Coherent lasers can be shown to have a Poisson output distribution, i.e., the number of photons produced by a coherent laser in a given time interval is a Poisson random variable. On the other hand, a Chaotic light source produced by a blackbody radiation can be shown to have a Bose-Einstein output statistic and coherent laser sources amplified by an optical amplifier can be shown to have Laguerre output statistics. Although output process of noncoherent sources are not readily modeled by a Poisson distribution, it can be shown that photon count of these sources can be well approximated with a Poisson process assuming that the number of temporal modes is much greater than one, i.e., counting is performed on a time interval much greater than laser's coherence time. Therefore, we will use a Poisson process to model the output of photodetected light source. Although we have used the Poisson distribution model for the received signal, the analysis does not depend particularly on this choice and can be easily used for models other than Poisson that are more precise. Counting the number of photons in a photon stream will be performed through counting the released photoelectrons at the output of the photodetector. Therefore, we expect a Poisson process at the output of a photodetector. These photoelectrons get trapped in a capacitor or an integrating circuit and produce an output voltage proportional to the number of released photoelectrons.

A Poisson random variable can be fully specified with the knowledge of its mean value. If mean of a Poisson process is m, then probability of count k is

$$p(k) = \text{Pos}(k, m) = e^{-m} \frac{m^k}{k!}. \tag{1}$$

If energy E has been emitted to a photodetector with quantum efficiency η, then mean number of photoelectron count at the output of the photodetector will be $m = E\eta/hf$ where f is frequency of light and h is Planck's constant.

Characteristic function of a Poisson random variable with distribution in (1) is $E(e^{sk}) = \exp\lfloor m(e^s - 1)\rfloor$. Dark current of photodetector can also be modeled as a Poisson process. In fact, Poisson distribution is the discrete equivalent of Gaussian distribution and Central Limit Theorem (CLT) in discrete cases can be shown to be valid for Poisson distribution. Therefore, processes like dark current which are the summation of a large number of independent discrete random variables can be well expressed by a Poisson distribution. It should be noted that the summation of independent Poisson random variables is itself a Poisson random variable. Therefore, the output current of a photodetector including dark current can be modeled as a shot-noise process, where the number of electrons in each time interval has a Poisson distribution. Practically, in order to count the number
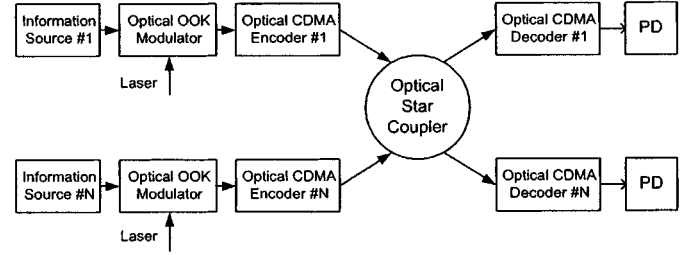

Fig. 1. Structure of a typical optical CDMA network.

of released photoelectrons; output current of photodetector will be integrated in a given time interval. During this integration process, a Gaussian circuit noise will be added to the output voltage of the integrator, where is usually proportional to the accumulated charge in a capacitor. Therefore, output voltage of the integrator is a compound Poisson and Gaussian process. Note that since this analysis is for a fiber-optic based network, background noise is weak and is not considered in this analysis. However, it can easily be added to the analysis. We have not also considered the dispersion effect imposed by traveling of short pulses on the length of fiber.

III. FIBER-OPTIC CDMA NETWORKS

Fig. 1 shows a typical structure of a fiber-optic CDMA network. Each information source provides an information bit for a laser based optical OOK modulator every T second. Pulses generated by an optical OOK modulator have duration $T_c = T/F$ where F is CDMA code length or processing gain of the system.

In an optical CDMA encoder, energy of pulses generated by data modulator splits into K (Code Weight) equal parts. Each part undergoes a pre-specified delay and then recombine in such a way to form the CDMA code pattern at the output of a CDMA encoder. This process is usually performed using optical couplers and optical tapped delay lines. We assume that OOC codes with minimum auto and cross-correlation is assigned to each user's encoder [1].

We denote by N, the number of active users of the network and by $N_{\max}$ the maximum number of allowed users, i.e., $N_{\max}$ is the size of the star coupler. Under conditions of minimum auto and cross-correlation, $N_{\max}$ is limited to $(F - 1)/K(K - 1)$ [1].

Star coupler, which is at the heart of the network, distributes the signal from each input port equally between its $N_{\max}$ output ports. At the receiver, a copy of the desired signal along with the interference from all other $N - 1$ active users will be received, and the receiver should be able to decide which bit of the desired user has been sent. BER performance of the receiver is highly affected by the architecture of CDMA decoder. We have shown eight different receiver structures for fiber-optic based CDMA using OOC in Fig. 2(a)–(h). In the remainder of this section, we will consider different receiver structures proposed for fiber-optic CDMA and discuss their major strengths and drawbacks. The receiver structures introduced and studied here are those structures with minimum electronic processing. The main electronic functions used in these structures are integration and comparison against a threshold value. These are the simplest electronic functions that can be implemented with relatively high
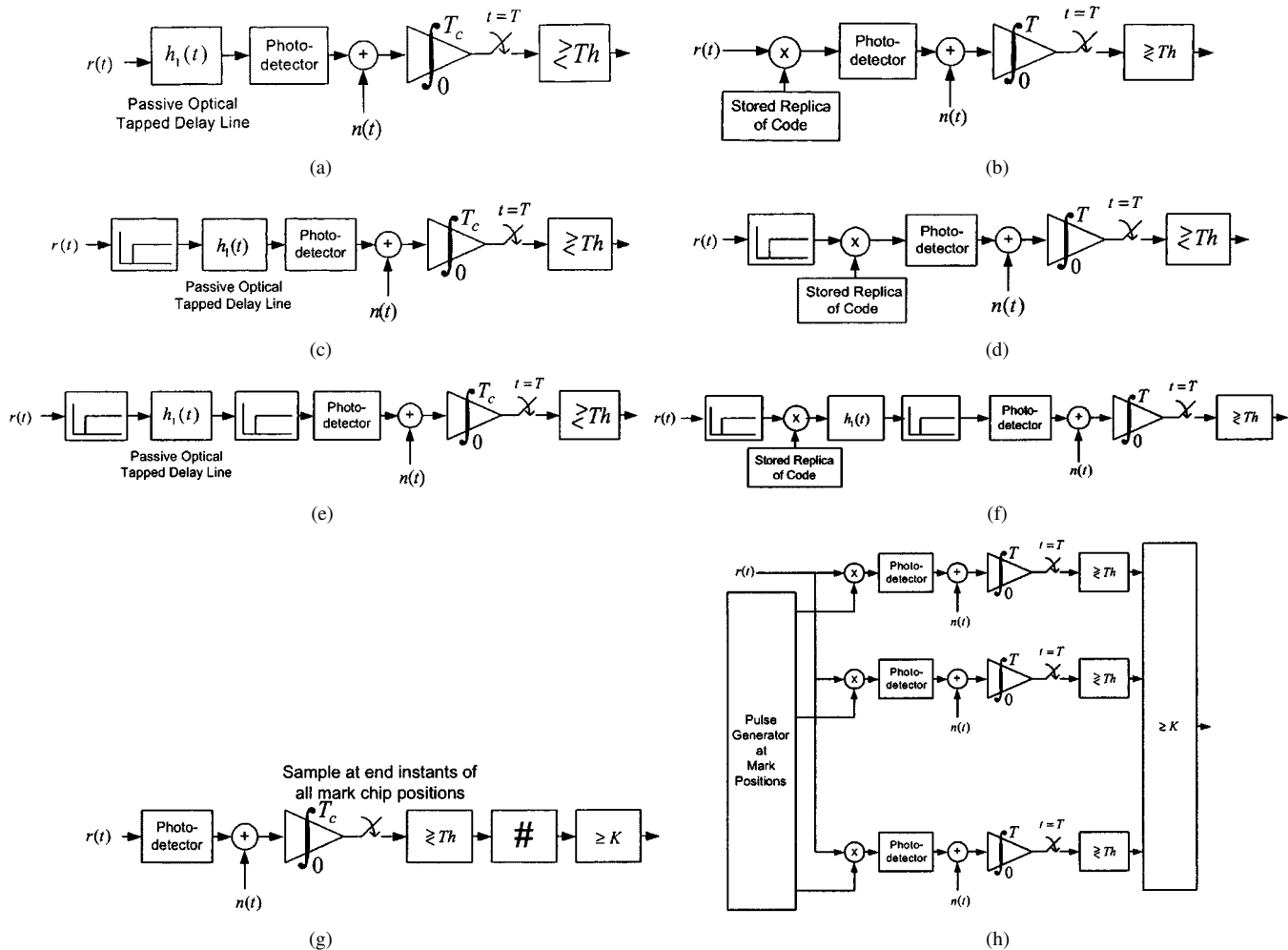
Fig. 2   (a) Passive correlator structure. (b) Active correlator structure. (c) Hard-limiter + passive correlator. (d) Hard-limiter + active correlator. (e) Double optical hard-limiter + passive correlator. (f) Double optical hard-limiter + double correlator. (g) High-speed chip-level detector. (h) Optical chip-level detector.

speeds. Other receiver structures can be introduced which massively benefit from electronic signal processing. Such receivers can employ for example pattern recognition or multi-user detection techniques to improve performance of the systems. However, the intensive electronic processing required is not desirable for high-speed optical CDMA signal processing due to its complexity.

A. Passive Correlation Receiver

In this receiver, received signal will be compared against transmitter signature sequence. The whole receiver performs match filtering on the input signal. Incoming signal will be divided into K equal parts each undergoing a time delay complement to one of delay elements of CDMA encoder to form a filter inversely matched to the transmitted signature sequence. For example, if $F = 32$ and transmitter sequence is (1, 4, 13, 30), then delay elements will be designed to generate delays $(31T_c, 28T_c, 19T_c, 2T_c)$. Output of these K delay lines will be combined and after photodetection and integration, output voltage will be sampled at the end of each bit interval. If transmitted bit is "One", an optical pulse will appear at the sampling chip-time with a power that is K times the power of each incoming chip pulse.

The major strength of this design is its passive optical correlator, however, this receiver needs a very high-speed electronic circuitry which should operate at a chip-rate speed which limits this structure and similar structures using passive correlator, only to relatively low-speed applications. Another drawback of this system is the strong power loss in optical splitters. The original pulse will split to K parts at the encoder and then each pulse will be divided to $N_{\max}$ parts at the star coupler and again to K parts at the optical decoder. Therefore, energy of original transmitter encoded laser pulse, will be divided to $N_{\max}K^2$ and forms the energy of each chip pulse at the receiver.

Hence, transmitter should produce strong enough pulses so that decision variable has enough energy for reliable decision. The sampled value, which is the output voltage of an integrator, will be compared against a threshold level Th and an estimation of the transmitted bit will be given.

B. Active Correlation Receiver

This receiver performs the same operation as passive correlation receiver, but an active multiplier that can be implemented for example using an acousto-optic modulator will perform code multiplication. Therefore, integration time after photodetector should be extended to T seconds and this receiver has a lower

speed electronic design comparing with passive correlation receiver, but uses a more complicated optical technology.

Using an active multiplier, only pulses at mark positions will enter the receiver and therefore integration should be performed over a bit time T. Therefore, this receiver needs electronic circuitry in bit-rate speed, not chip-rate speed, which is more feasible than electronic circuit in passive correlation structure. This structure is also more efficient regarding required power and does not split the received power like as in passive correlator. However, the receiver need an optical multiplier which itself has speed limitations and is a costly device.

C. Optical Hard-Limiter + Passive Correlation Receiver

This structure removes many interference patterns using an optical hard-limiter before correlation receiver of Fig. 2(a) [2].

The function of an optical hard-limiter at the input of correlator is to limit the energy of input pulses to the equivalent of one pulse. Therefore, if transmitted bit is "zero" and there are several interfering pulses at a specified mark position, the optical hard-limiter, limits the incoming optical energy to the energy of just one pulse. Therefore, number of input pulses to the correlator is limited to one pulse at each chip time position, thus considerably reduces the possibility of detecting "one" when "zero" has been transmitted.

For example, if $K = 4$ and transmitted bit is "zero", assume that number of received pulses at four positions are (3, 2, 0, 0). A correlation receiver adds these numbers, compares the result with K, and erroneously decides that bit "one" is transmitted. However, a hard-limiter converts the interference pattern to (1, 1, 0, 0) allowing the correlator a sufficient margin to make a correct decision about the transmitted bit.

D. Optical Hard-Limiter + Active Correlation Receiver

This receiver uses a hard-limiter before active correlation receiver. Therefore, this structure needs a lower speed electronic technology.

Again, many interference patterns that could produce error in simple correlation receiver are omitted because of the use of hard-limiter. Integrating time of the receiver has been extended by use of an optical multiplier instead of a passive correlator. Although longer integration times makes the design of the receiver simpler, but it adds to the collected dark current at the receiver and increases BER of the system.

E. Double Optical Hard-Limiter + Passive Correlation Receiver

Double optical hard-limiter structure removes many interference patterns, which will pass through a simple optical hard-limiter.

The first hard limiter clips the energy of incoming pulses, but the second hard-limiter removes the stray pulses produced by passive optical correlator (delay lines) not contributing to the decision criteria. For example, consider the optical hard-limiter structures of Figs. 2(c) and (d). If there is no statistical quantum behavior in photodetector, i.e., no shot noise, the ideal threshold value is K times the number of received photons in a clipped chip.

Since this may not be a practical and a realistic assumption, optimum threshold is well below this value and it could be, for example, equal to half this amount. Therefore, each interference pattern that can provide the photodetector with more than this number of photons will result in an error if transmitted bit is "zero". In double optical hard-limiter, only interference patterns that have pulses exactly at all K mark positions can produce errors if transmitted bit is "zero".

F. Double Optical Hard-Limiter + Double Correlation Receiver

This structure is an alternate structure for receiver in Fig. 2(e) where a lower speed electronic is required. The first hard-limiter clips the energy of incoming pulses and therefore reduces the incoming interference, but the second hard-limiter omits the stray pulses produced by optical correlator and can only pass the correlation component. In fact, the second hard-limiter has the task of optically deciding about transmitted bit and remaining circuitry of receiver only has the task of converting this optical decision into an electrical signal.

In order to increase integration time in double optical hard-limiter, an active multiplier has been used before passive correlator in Fig. 2(e). The multiplier removes interference received in space chip positions. Then passive correlator accumulates energy received in mark chip positions. Therefore, integration time can be extended from T_c up to T. In fact, integration time is not necessarily T and each time interval that contains peak correlation chip-time can be chosen to be the integration time. Although longer integration times makes the electronic circuits more feasible, but it increases the contribution of collected noise in decision variable. Therefore, shorter integration times are preferable and this integration time is better to be reduced to as much as possible, e.g., down to T_c.

It should be noted here that the proposed receiver structures in Fig. 2(e) and (f) are equivalent to the variations of an earlier proposed receiver structure based on optical AND gates [8].

G. High-Speed Chip-Level Detector

Fig. 2(g) shows the block diagram of a chip-level receiver. In this receiver, decision is based on K partial decision random variables. Signal will be sampled at each chip pulse interval and a "one" bit will be detected when at least one pulse is present at all chip pulse positions and a single missed chip pulse at the designated code pulse position is sufficient to detect "zero" bit. It can be shown that if no noise is present, hard-limiter receiver performs as well as chip-level detector.

This receiver requires a fast electronic design, since the receiver needs to integrate K times the incoming signal on T_c intervals during a bit time. It has been shown that if only Poisson Shot-Noise is considered, the performance of this receiver rapidly approaches the performance of ideal hard-limiter receiver [6].

H. Optical Chip-Level Detector

This is an alternate structure for receiver in Fig. 2(g) that requires a lower speed electronic design. Each branch of the receiver independently decides whether a pulse has been sent in

a specified chip position or not. Ideally, receiver decides a bit "one" only if a mark is detected in all chip positions. Again integration times can be reduced down to T_c.

It should be noted that when there is no noise present, performance of receiver structures in Fig. 2(c)–(h) is the same and their performances in multi-access limited conditions, i.e., when photodetector and decision circuit add no noise is limited to results in [2] for single hard-limiter structure.

In the analysis that follows, we have assumed that optical hard-limiters operate based on energy of the incoming signal in each chip time. In fact, we have neglected the effect of statistical photon emission properties of optical sources and optical hard-limiters. It can be shown that this assumption is true if mean number of incoming photons per pulse is greater than approximately 20. Therefore, if received energy per chip pulse is not too low, quantum properties of source on optical hard-limiter can be neglected. Practical high-quality optical hard-limiters are not available yet. However, results of research on optical nonlinear elements are promising enough to consider optical hard-limiters even before they are practically realized.

IV. BER PERFORMANCE ANALYSIS

In this analysis, we assume that different signals are frame asynchronous, i.e., no effort has been made to synchronize different transmitters. Analysis of BER of such a system seems to be quite intractable. A simplifying assumption is to consider different signals to be chip synchronous. This is a pessimistic case and gives an upper bound to the BER of the real asynchronous system [1].

We adopt the notation in [5] to model the interference patterns. We denote by α_j, $j = 1, 2, \ldots, K$ the number of interfering pulses received in jth pulse position and by $\vec{\alpha} = (\alpha_1, \alpha_2, \ldots, \alpha_K)$ the vector of received interference. In OOC with minimum Auto- and Cross-Correlation, two codewords cannot overlap at more than one pulse position. Since each code word has K pulses, there are K^2 ways of pairing the K pulses of two users. Therefore, the probability that two code words overlap at one pulse position is $q = K^2/2F$ where factor $1/2$ accounts for the probability that interfering user has sent "one". Assuming $N - 1$ interfering users, the probability that there are l interfering pulses is given by

$$\Pr(l) = \binom{N-1}{l} q^l (1-q)^{N-1-l} \quad l = 0, 1, \ldots, N-1.$$

(2)

Assuming l interfering pulses, there is a set of interference patterns so that $\sum_{i=1}^{K} \alpha_i = l$. We denote this set of vectors with F_l. Since l interfering users are distinguishable, they can produce K^l interference patterns. However, what is important for decision at receiver is vector $\vec{\alpha}$ not the specific users who have produced the interference pattern. Assuming l interfering pulses, pattern $\vec{\alpha}$ can be produced in

$$\binom{l}{\alpha_1, \alpha_2, \ldots, \alpha_K} = \binom{l}{\alpha_1} \binom{l - \alpha_1}{\alpha_2} \ldots \binom{\alpha_K}{\alpha_K}$$

$$= \frac{l!}{\prod_{i=1}^{K} \alpha_i!}$$

ways each with probability $1/K^l$. Therefore, if $P_E(\vec{\alpha})$ is the probability of error given interference pattern $\vec{\alpha}$, then error probability can be expressed as

$$P_E = \sum_{l=0}^{N-1} \Pr(l) P_E(F_l)$$

(3)

where from [5]

$$P_E(F_l) = \sum_{\vec{\alpha} \in F_l} \frac{l!}{K^l} \frac{P_E(\vec{\alpha})}{\prod_{i=1}^{K} \alpha_i!}$$

(4)

where $P_E(\vec{\alpha})$ depends on receiver structure as well as interference pattern $\vec{\alpha}$. F_l is a set of $(l + K - 1)!/l!(K - 1)!$ vectors, and generating and calculating their associated error probabilities could be quite computationally intensive which makes the scheme impractical. We will find simplifying formulas for BER calculation depending on special receiver structure. $P_E(\vec{\alpha})$ in each case not only depends on receiver structure, but also on photodetection parameters like signal power, noise power, and quantum efficiency of photodetector.

We assume a circuit noise with a power spectrum density $N_0(A^2/Hz)$, and the variance of the output noise of an integrator with integration duration of T seconds will be $\sigma^2 = N_0 T/2$ [3]. We denote by λ_d the dark current photoelectron rate of the photodetector. Therefore, mean of photoelectron count over a period of T seconds will be $\lambda_d T$. We also denote by λ_s the rate of photoelectron count due to a single chip pulse in receiver. λ_s depends on transmitter power, K (code weight), receiver structure and quantum efficiency of the photodetector. We also assume that energy E_s is transmitted per OOK pulse. This energy will be divided into K equal parts in CDMA encoder and further will be divided into $N_{\max}$ equal parts in the star coupler.

A. Passive Correlation Receiver

In this receiver, filter $h_1(t)$ is a set of passive optical tapped delay lines. Input pulse will be divided into K equal parts. Therefore, λ_s can be expressed as $\lambda_s = \eta E_s/(N_{\max} K^2 T_c hf)$. In this receiver, $P_E(\vec{\alpha})$ depends on $\sum_{i=1}^{K} \alpha_i = l$ not just on the specific pattern $\vec{\alpha}$. Hence, $P_E(F_l) = P_E(\vec{\alpha})$ and can be expressed as

$$P_E(\vec{\alpha}) = \frac{1}{2} P_E(\vec{\alpha} \mid 0) + \frac{1}{2} P_E(\vec{\alpha} \mid 1)$$

$$= \frac{1}{2} \int_{\text{Th}}^{\infty} P_{v_t}(v \mid 0, \vec{\alpha}) \, dv + \frac{1}{2} \int_{-\infty}^{\text{Th}} P_{v_t}(v \mid 1, \vec{\alpha}) \, dv$$

(5)

where

$$P_{v_t}(v \mid b, \vec{\alpha}) = \sum_{n=0}^{\infty} P(n \mid b, \vec{\alpha}) \left[\frac{\exp[-(v - e_0 n)^2/2\sigma^2]}{\sqrt{2\pi\sigma^2}} \right]$$

(6)

where b represents transmitted bit and $\sigma^2 = N_0 T_c/2$ and e_0 is the charge of an electron. $P(n \mid b, \vec{\alpha})$ can be expressed as:
$P(n \mid b, \vec{\alpha}) = \text{Pos}(n, ((Kb + l)\lambda_s + \lambda_d)T_c)$.

B. Active Correlation Receiver

In this receiver, $\lambda_s = \eta E_s/N_{\max}KT_chf$. BER of this receiver follows (5) and (6) where $\sigma^2 = N_0T/2$ and $P(n\,|\,b,\vec{\alpha}) = \text{Pos}(n,(Kb+l)\lambda_sT_c + \lambda_dT)$.

C. Hard-Limiter + Passive Correlation Receiver

In this receiver, number of nonzero elements of $\vec{\alpha}$ which we denote it by $|\vec{\alpha}|$ is the effective interference parameter. In other words, $P_E(\vec{\alpha}) = P_E(\beta)$ iff $|\alpha| = |\rho|$. Therefore, P_E can be expressed as

$$P_E = \sum_{c=0}^{K} \text{Pr}\{|\vec{\alpha}| = c\}P_E(\vec{\alpha}). \qquad (7)$$

In the Appendix, we will prove that

$$\text{Pr}\{|\vec{\alpha}| = c\} = \binom{K}{c}\sum_{i=0}^{c}(-1)^i\binom{c}{i}$$
$$\times \left(1 - (K-c+i)\frac{K}{2F}\right)^{N-1}. \qquad (8)$$

In this receiver $\lambda_s = \eta E_s/N_{\max}K^2T_chf$ and optical hard-limiter clips the energy of pulses to $E_s/N_{\max}K$ and vanishes pulses with less energy. $P_E(\vec{\alpha})$ can be expressed by (5) and (6) where $\sigma^2 = N_0T_c/2$ and $P(n\,|\,b,\vec{\alpha}) = \text{Pos}(n,\{(Kb+(1-b)|\vec{\alpha}|)\lambda_s + \lambda_d\}T_c)$.

D. Hard-Limiter + Active Correlation Receiver

In this receiver $\lambda_s = \eta E_s/N_{\max}KT_chf$ and optical hard-limiter clips the energy of pulses to $E_s/N_{\max}K$ and vanishes pulses with less energy. $P_E(\vec{\alpha})$ can be expressed by (5) and (6) where $\sigma^2 = N_0T/2$ and $P(n\,|\,b,\vec{\alpha}) = \text{Pos}(n,(Kb+(1-b)|\vec{\alpha}|)\lambda_sT_c + \lambda_dT)$..

E. Double Optical Hard-Limiter + Passive Correlator Receiver

In this case, error occurs when transmitted bit is "one" but receiver fails to detect the transmitted bit, because of quantum noise effects or circuit noise. The other case is that when transmitted bit is "zero" and decision criteria passes the threshold value because of interfering users or dark current or circuit noise. Probability of error can be expressed by (5), (6), (7), and (8) where $\sigma^2 = N_0T_c/2$ and $\lambda_s = \eta E_s/N_{\max}K^2T_chf$ and $P(n\,|\,b,\vec{\alpha})$ can be expressed in the first equation shown at the bottom of the page. The optical hard-limiters clip the energy of incoming pulses to $E_s/N_{\max}K$.

F. Double Optical Hard-Limiter + Double Correlator Receiver

In this receiver, $\lambda_s = \eta E_s/N_{\max}K^2T_chf$. Probability of bit error can again be expressed by (5), (6), (7), and (8) with $\sigma^2 = N_0T/2$ and the second equation shown at the bottom of the page. The optical hard-limiters clip the energy of incoming pulses to $E_s/N_{\max}K$.

G. High-Speed Chip-Level Detector

In this receiver, $\lambda_s = \eta E_s/N_{\max}KT_chf$. Output voltage of each integrator will be compared to a threshold voltage Th. We note that if $\vec{\alpha}$ and β are permutations of each other, then $P_E(\vec{\alpha}) = P_E(\beta)$. Therefore, in order to calculate $P_E(F_l)$, it is not necessary to generate all vectors in F_l. We define a new set G_l so that elements of G_l are nonincreasing elements of F_l, i.e., $\vec{\alpha} \in G_l$ iff $\vec{\alpha} \in F_l$ and $\alpha_1 \geq \alpha_2 \geq \cdots \geq \alpha_K \geq 0$. Number of permutations of vector $\vec{\alpha}$ can be expressed by $N(\vec{\alpha})$ where

$$N(\vec{\alpha}) = \frac{K!}{\prod_i R(\alpha_i)!}$$

where $R(\alpha_i)$ is number of repetitions of α_i in $\vec{\alpha}$ and the product is taken over i for which α_i are distinct. Therefore, $P_E(F_l)$ can be expressed as

$$P_E(F_l) = \sum_{\vec{\alpha}\in G_l} \frac{l!N(\vec{\alpha})P_E(\vec{\alpha})}{K^l\prod_{i=1}^{K}\alpha_i!}$$

elements of G_l can be generated using the following recursive algorithm. Procedure $make(m,l,n)$ when called from main program with elements $m = K, l = l, n = 0$, generates all vectors with length K and weight l and places the generated vectors in vector A which can be used for calculation of BER.

```
Procedure make(m, l, n)
{
    if (l = 0)
        for j = 0 . . . n
            for i = 0 . . . B[j]
                A[i] = A[i] + 1
    else
        for i = 1 . . . min(m, l)
        {
            B[n] = i
            make(i, l − i, n + 1)
        }
}
```

$$P(n\,|\,b,\vec{\alpha}) = \begin{cases} \text{Pos}(n,(K\lambda_s + \lambda_d)T_c) & (b=1) \text{ or } (b=0,|\vec{\alpha}|=K) \\ \text{Pos}(n,\lambda_dT_c) & (b=0,|\vec{\alpha}|<K) \end{cases}.$$

$$P(n\,|\,b,\vec{\alpha}) = \begin{cases} \text{Pos}(n,(K\lambda_sT_c + \lambda_dT) & (b=1) \text{ or } (b=0,|\vec{\alpha}|=K) \\ \text{Pos}(n,\lambda_dT_c) & (b=0,|\vec{\alpha}|<K) \end{cases}.$$

Vector B in this program segment should be a global vector. $P_E(\vec{\alpha})$ can be calculated as follows:

$$
\begin{aligned}
P_E(\vec{\alpha}) &= \frac{1}{2} P_E(\vec{\alpha} \,|\, 0) + \frac{1}{2} P_E(\vec{\alpha} \,|\, 1) \\
&= \frac{1}{2} \prod_{i=1}^{K} \Pr(v_i \geq \mathrm{Th} \,|\, \alpha_i, b = 0) \\
&\quad + \frac{1}{2} \left(1 - \prod_{i=1}^{K} \Pr(v_i \geq \mathrm{Th} \,|\, \alpha_i, b = 1) \right) \quad (9)
\end{aligned}
$$

where v_i is the output of i'th integrator and

$$
\begin{aligned}
&\Pr(v_i \geq \mathrm{Th} \,|\, \alpha_i, b) \\
&= \sum_{n=0}^{\infty} P(n \,|\, \alpha_i, b) \left[\frac{\exp[-(v - e_0 n)^2 / 2\sigma^2]}{\sqrt{2\pi\sigma^2}} \right] \quad (10)
\end{aligned}
$$

where $\sigma^2 = N_0 T_c / 2$ and $P(n \,|\, b, \alpha_i) = \mathrm{Pos}(n, \{(b + \alpha_i)\lambda_s + \lambda_d\}T_c)$. It can be seen that $\Pr(v_i \geq \mathrm{Th} \,|\, \alpha_j, b)$ is a function of $b + \alpha_i$ which ranges from zero to $N + 1$. Therefore, it is sufficient to calculate once all $N + 2$ possible values of (10) for each specific set of values of $\lambda_s, \lambda_d, \sigma$, store them in an array and then use these pre-stored values to calculate (9).

H. Optical Chip-Level Detector

In this receiver, $\lambda_s = \eta E_s / N_{\max} K^2 T_c h f$. $P_E(\vec{\alpha})$ can be expressed by (9) and (10) where $\sigma^2 = N_0 T / 2$ and $P(n \,|\, b, \alpha_i) = \mathrm{Pos}(n, (b + \alpha_i)\lambda_s T_c + \lambda_d T)$.

V. NUMERICAL RESULTS

Numerical evaluation of (5) and (6) can be quite time consuming and needs high-precision variables and calculation. Because of very small values of BER, calculation using ordinary precision variables can make erroneous results.

We have used saddle-point approximation method in order to compute the numerical values of these equations. In order to evaluate (5) using saddle-point approximation method, characteristic function of random variable v_t (accumulated charge in the integrator) should be evaluated. Conditioned on transmitted bit and interference pattern $\vec{\alpha}$, random variable v_t is the summation of a circuit Gaussian noise sample with variance σ^2 and the total charge of released photoelectrons. σ^2 is the variance of accumulated charge in the integrator due to circuit noise. Charge of each electron is e_0 and number of photoelectrons is a random variable with Poisson distribution. Therefore, characteristic function of compound random variable v_t assuming that the number of photoelectrons N has a Poisson distribution with mean K_s can be expressed as

$$
\Phi(s) = \phi_{v_t \,|\, b, \vec{\alpha}}(s) = E(e^{v_t s}) = e^{K_s(e^{e_0 s} - 1)} e^{s^2 \sigma^2 / 2}
$$

a new function $\psi(s)$ is defined where

$$
\begin{aligned}
\psi(s) &= \ln \frac{\Phi(s) e^{-\mathrm{Th} \cdot s}}{s} \\
&= K_s(e^{e_0 s} - 1) + \frac{s^2 \sigma^2}{2} - \mathrm{Th} \cdot s - \ln|s| \quad (11)
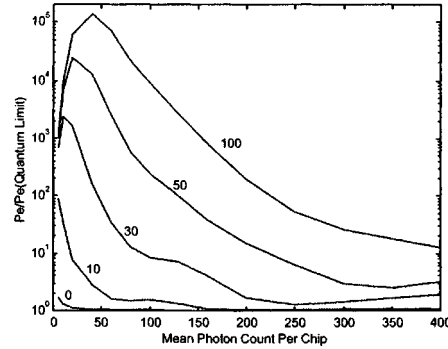\end{aligned}
$$

Fig. 3. Performance degradation of correlation receiver with respect to quantum limit condition due to circuit noise for several values of σ_n versus mean photon count per chip, $\lambda_s T_c$ and for $i_d = 160.1\ \mathrm{nA}(\lambda_d T_c = 5)$.

Positive and negative roots of equation $\psi'(s) = 0$ are called s_0 and s_1 respectively. Saddle-Point approximation states that [4]

$$
\begin{aligned}
\int_{\mathrm{Th}}^{\infty} P_{v_t}(v \,|\, b, \vec{\alpha})\, dv &\approx \frac{\exp[\psi(s_0)]}{\sqrt{2\pi\psi''(s_0)}} \\
\int_{-\infty}^{\mathrm{Th}} P_{v_t}(v \,|\, b, \vec{\alpha})\, dv &\approx \frac{\exp[\psi(s_1)]}{\sqrt{2\pi\psi''(s_1)}}
\end{aligned}
$$

We assume a CDMA system with $R_b = 100$ Mb/s per user. We also assume that OOC codes with code length $F = 2000$ and $K = 9$ weight with $N_{\max} = 27$ has been used. We also assume that photodetector dark current is $i_d = 160$ nA which is a typically high value for dark current noise. Therefore, mean dark current electron count in each chip time interval ($T_c = 5$ ps) would be $m_d = 5$. We assume that system is operating at 1.55 μm and photodetector quantum efficiency is $\eta = 0.8$.

For variance σ^2 of the thermal circuit noise added to the output of the receiver, we will use instead parameter $\sigma_n = \sigma / e_0$ which is the normalized value of the standard deviation.

The results of BER in each condition and for each structure of receiver have been derived for optimum threshold and its value is obtained by trial and error.

Performance degradation of receiver with a structure of Fig. 2(a) versus mean photon count per chip is shown in Fig. 3 for several values of σ_n. The base for performance degradation is quantum limit condition, i.e., no circuit and dark current noise. It can be seen that performance degradation due to circuit noise can be quite sever especially when the received signal is very low power. Note that the curve for $\sigma_n = 0$ is representative of a CDMA system with shot-noise and dark current. It can be seen that there is a minute performance degradation due to dark current when signal is low power, so that number of received photons in a bit is comparable with dark current electron count on that time interval. As σ_n increases, more photons is needed to overcome the randomness effect caused by circuit Gaussian noise. Performance degradation due to circuit noise may become even more sever for other receiver structures. The receiver in Fig. 2(a) uses a chip time integrator. Hence, the contribution of dark current noise and Gaussian noise will be quite less than those receiver structures which employ bit time integrator. In other words, for a given λ_d and N_0, variance of
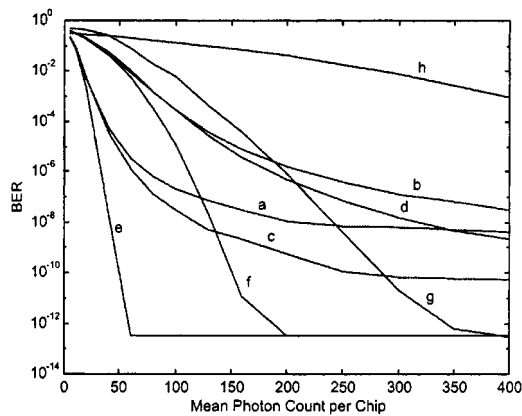
Fig. 4. Dependence of BER on mean photon count per chip, $\lambda_s T_c$, for various receiver structures, $\sigma_n = 30$, $\lambda_d T_c = 5$.

Fig. 5. Dependence of BER on transmitter peak power for various receiver structures, $\sigma_n = 30$, $\lambda_\delta T_c = 5$.

the associated noises at the output of the bit time integrator will be much more than the chip time integrators. In such receivers, contribution of enumerated electrons due to dark current and enumerated electrons due to Gaussian circuit noise in decision variable will be multiplied by F/K in respect to receiver structures with chip time integration.

Dependence of BER on mean photon count per chip is depicted in Fig. 4 for different receiver structures. We have assumed $\sigma_n = 30$ which is a typical value for receivers with chip-time integrators. Typical values of σ_n for receivers employing bit time integrators is much higher. In order to compare the behavior of different systems against Gaussian circuit noise, it is better to take N_0 as a constant, but our purpose is to demonstrate the behavior of each system with increasing received power. We have assumed that number of simultaneous users is 25. It can be seen that double optical hard-limiter BER approaches very fast to the ideal no noise BER. On the other hand, the effect of circuit noise on the performance of optical chip-level receiver is quite severing. Structure of Fig. 2(h), which performs very well in quantum-limit conditions [6], has a very poor performance when dark current noise and Gaussian circuit noise is considered. Effectiveness of optical hard-limiter can be seen in the reduction of interference patterns by comparing curves of BER for structures Fig. 2(a) and (c), Fig. 2(b) and (d). However, improvement is not as promising as reported in [2] with the use of a single hard-limiter and this furthermore confirms the same conclusions made in [9]. The improvement predicted in [2] using a single hard-limiter can only be reached for high received power and when all signal dependent randomness effects are removed.

Average transmitter power can be related to E_s by $P_a = E_s/2T_b$ and receiver peak power can be expressed by $P_p = E_s/T_c = 2P_a F$. BER of various structures versus transmitter peak power is depicted in Fig. 5. This figure indicates relative effectiveness of different structures while considering transmitter power. This figure shows that receivers employing passive correlator perform worse than their counterparts with active correlator from the point of view of required transmission power. The required high value for transmitter peak power shows that selection of laser source and receiver structure should be performed carefully in order to provide the receiver with sufficient power.
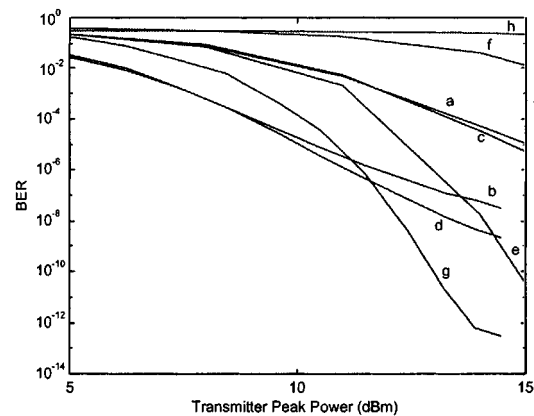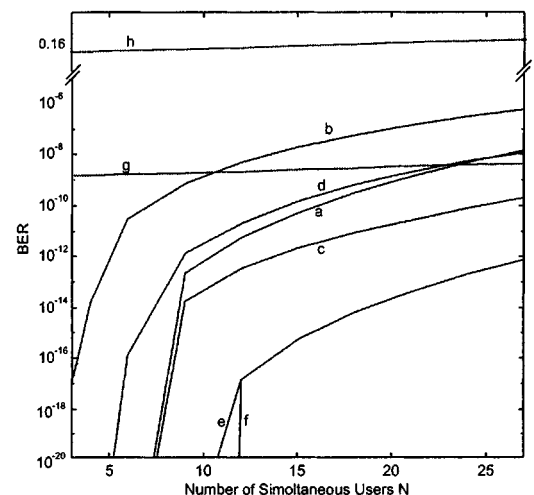

Fig. 6. Dependence of BER on number of simultaneous users of the network, N, for various receiver structures, $\sigma_n = 30$, $\lambda_d T_c = 5$, $\lambda_s T_c = 250$.

Noting that the typical value σ_n of could be much higher for receivers with bit time integration, the required transmitter power may be unacceptably high. Therefore, it seems that the use of optical amplifiers in optical CDMA systems is inevitable [10].

Finally, the effect of number of simultaneous users on the performance of the system is shown in Fig. 6 for various receiver structures. Mean received photon count per chip time is considered fixed for each receiver structure. The main noticeable point about this figure is the relative flatness of performance of chip-level detectors with the number of simultaneous users. This is mainly because of strength of chip-level detectors in detecting error patterns caused by interfering users. This capability remains while the number of users approaches its maximum and therefore with the increase of the number of users there is only a slight degradation in the performance of chip-level detectors. Ideal optical CDMA systems may behave error-free when number of users is less than code weight K [2], since all the interfering users altogether cannot produce an interference pattern with sufficient power. However, such an effect cannot be implemented when other noise sources are considered. Because of shot-noise effect, there is also a probability of missed-detection that is in contrast with ideal system where there is only

TABLE I
COMPARISON OF VARIOUS OPTICAL CDMA RECEIVER STRUCTURES

Receiver Design	Integration Time	Electronic Bandwidth	Receiver Complexity	Notes on Overall Usability and relative strength/weakness
(a)	T_c	Large	Low	Low-Speed applications, inefficient power consumption, inexpensive
(b)	T	Low	Moderate	High-Speed applications, relatively expensive design
(c)	T_c	Large	Moderate	Low-Speed applications, depends on the availability of Optical Hard-Limiter
(d)	T	Low	Moderate	High-Speed applications, depends on the availability of Optical Hard-Limiter
(e)	T_c	Large	Moderate	Low-Speed applications, Excellent Performance, relatively expensive
(f)	$\geq T_c, \leq T$	Medium-Large	High	Medium to High Speed applications, inefficient power consumption
(g)	T_c	Large	Low	Low-Speed applications, efficient power consumption
(h)	$\geq T_c, \leq T$	Medium-Large	High	Unusable

false-alarm probability. Therefore, threshold value cannot be set too high in order to avoid missed-detection and this causes the system to suffer both from false-alarm and missed-detection probabilities and the receiver cannot reach error-free conditions even when the number of users is less than code weight. Again, double-optical hard-limiter systems have the closet performance to the ideal systems and their BER drops very quickly when number of users is less than code weight.

Table I summarizes comparison of receiver designs and relative strength and weaknesses of the special designs.

VI. CONCLUSION

In this paper, we studied the performance of fiber-optic CDMA systems employing OOCs using various receiver structures. We introduced a unifying methodology in evaluating the performance of vastly different receiver structures. Our results show that the most feasible receiver structure, i.e., correlation receiver cannot operate easily without the use of an optical amplifier. The use of optical hard-limiters can improve the performance of the system. We showed another important factor in the effectiveness of different receiver structures to be the integration time. Shorter integration times gives better performance results. Therefore, introduction of optical hard-limiters and high-speed integrate and dump circuits are two important factors which make power efficient fiber-optic CDMA receivers realizable.

APPENDIX

In this Appendix, we obtain (8). Translating this problem into the familiar problem of balls and boxes, we are confronted with this problem: We place l distinguishable balls into K equal boxes. $\Pr\{|\vec{\alpha}| = c \,|\, l\}$ is the probability that exactly c out of K boxes are filled. We will denote by $S(l, K, c)$ the number of ways that only c out of K boxes are filled with l distinguishable balls. We know from [5] that $S(l, K, K)$ is on the form of

$$S(l, K, K) = \sum_{i=0}^{K-1} (-1)^i \binom{K}{i} (K-i)^l$$

We note that $S(l, K, c) = \binom{K}{c} S(l, c, c)$. Therefore,

$$S(l, K, c) = \binom{K}{c} \sum_{i=0}^{c} (-1)^i \binom{c}{i} (c-i)^l$$

$$\Pr\{|\vec{\alpha}| = c\} = \sum_{i=0}^{N-1} \binom{N-1}{l} q^l (1-q)^{N-1-l} \frac{1}{K^l}$$

$$\times \binom{K}{c} \sum_{i=0}^{c} (-1)^i \binom{c}{i} (c-i)^l$$

$$= \sum_{i=0}^{c} \binom{K}{c} (-1)^i \binom{c}{i} \sum_{l=0}^{N-1} \binom{N-1}{l}$$

$$\times q^l (1-q)^{N-1-l} \frac{1}{K^l} (c-i)^l$$

$$= \binom{K}{c} \sum_{i=0}^{c} (-1)^i \binom{c}{i} \sum_{l=0}^{N-1} \binom{N-1}{l}$$

$$\times \left(\frac{q}{K}(c-i) \right)^l (1-q)^{N-1-l}$$

$$= \binom{K}{c} \sum_{i=0}^{c} (-1)^i \binom{c}{i}$$

$$\times \left[1 - (K-c+i)\frac{K}{2F} \right]^{N-1}$$

REFERENCES

[1] J. A. Salehi, "Code division multiple access techniques in optical fiber networks—Part I: Fundamental principles," *IEEE Trans. Commun.*, vol. 37, pp. 824–833, Aug. 1989.
[2] J. A. Salehi and C. A. Brackett, "Code division multiple access techniques in optical fiber networks—Part II: System performance analysis," *IEEE Trans. Commun.*, vol. 37, pp. 834–842, Aug. 1989.
[3] R. M. Gagliardi and S. Karp, *Optical Communications*. New York, NY: John Wiley, 1995.
[4] C. W. Helstrom, "Approximate evaluation of detection probabilities in radar and optical communications," *IEEE Trans. Aerosp. Electron. Syst.*, vol. AES-14, pp. 630–640, July 1978.

[5] M. Azizoglu, J. A. Salehi, and Y. Li, "Optical CDMA via temporal codes," *IEEE Trans. Commun.*, vol. 40, pp. 1162–1170, July 1992.

[6] H. M. H. Shalaby, "Chip-level detection in optical code-division multiple-access," *J. Lightwave Technol.*, vol. 16, pp. 1077–1087, June 1998.

[7] T. Ohtsuki, "Performance analysis of direct-detection optical asynchronous CDMA systems with double-optical hard-limiters," *J. Lightwave Technol.*, vol. 15, pp. 452–457, Mar. 1997.

[8] J. A. Salehi, "Emerging optical code-division multiple access communications systems," *IEEE Network Mag.*, vol. 3, pp. 31–39, Mar. 1989.

[9] H. M. Kwon, "Optical orthogonal code division multiple access system—Part I: With avalanche photodiode noise and thermal noise," *IEEE Trans. Commun.*, vol. 42, pp. 2470–2479, July 1994.

[10] M. Razavi and J. A. Salehi, "Fiber-optic CDMA networks incorporating multiple optical amplifiers," in *Proc. IEEE Globecom Conf.*, vol. II, Nov.–Dec. 2000, pp. 1247–1253.

Jawad A. Salehi (S'80–M'84) received the B.S. degree in electrical engineering from the University of California, Irvine, in 1979, and the M.S. and Ph.D. degrees from the University of Southern California (USC), Los Angeles, in 1980 and 1984, respectively.

From 1981 to 1984, he was a full-time Research Assistant at Communication Science Institute at USC engaged in research in the area of spread spectrum systems. From 1984 to 1993, he was a Member of technical staff with the Applied Research Area at Bell Communications Research (Bellcore), Morristown, NJ. From February to May 1990, he was with the Laboratory for Information and Decision Systems at the Massachussets Institute of Technology (MIT), Cambridge, as a Visiting Research Scientist conducting research on optical multiple-access networks. Currently, he is an Associate Professor with the Department of Electrical Engineering, Sharif University of Technology, Tehran, Iran, and since fall 1999, he has also been a Co-Director of Advanced and Wideband CDMA Lab at Iran Telecom Research Center (ITRC) conducting research in the area of advance CDMA techniques for optical and radio communications systems. His current research interests are in the areas of optical multi-access networks, in particular, fiber-optic CDMA, femtosecond or ultra-short light pulse CDMA, spread time CDMA, holographic CDMA, wireless indoors infrared CDMA systems, and applications of EDFA in optical systems. His work on optical CDMA systems resulted in ten U.S. patents.

Dr. Salehi is a recipient of the Bellcore's Award of Excellence. He assisted, as a member of the organizing committee, to organize the first and the second IEEE Conferences on Neural Information.

Sina Zahedi (S'98) was born in 1976. He received the B.S. and M.S. degrees (with honors) in electrical engineering from Sharif University of Technology (S.U.T.), Tehran, Iran, in 1998 and 2000. He is currently working toward the Ph.D. degree in the Department of Electrical Engineering at Stanford University, Stanford, CA.

From August 1999 to August 2000, he was a Member of Research Staff with Advanced CDMA Research Lab at Iran Telecommunication Research Center (ITRC), Tehran. His research interests are indoors infrared wireless communication systems, optical switches, optical networks and crossconnects, specifically, optical WDM and CDMA networks.